Radiationless Deactivation of the Second Excited Singlet State $^1\Sigma_g^+$ of O_2 in Solution

Reinhard Schmidt* and Marcus Bodesheim

Institut für Physikalische und Theoretische Chemie, J. W. Goethe-Universität, Marie-Curie-Str. 11, D60439 Frankfurt am Main, Germany

Received: February 17, 1998; In Final Form: April 6, 1998

The deactivation of the upper excited singlet oxygen $O_2(^1\Sigma_g^+)$ by 22 different quenchers has been studied in the liquid phase by time-resolved emission experiments. Radiationless deactivation occurs by electronic to vibrational (e−v) energy transfer to terminal bonds X−Y of the quenching molecule. A model is presented which describes the broad variation of rate constants over 4 orders of magnitude. The quantitative comparison with the e−v deactivation of $O_2(^1\Delta_g)$ demonstrates that for $O_2(^1\Sigma_g^+)$ in addition to the excitation of stretching modes the excitation of bending modes of X−Y becomes important for the overall deactivation process.

Introduction

There are two excited singlet states with excitation energies of 7882 ($a^1\Delta_g$) and 13 121 cm^{-1} ($b^1\Sigma_g^+$) closely lying above the $X^3\Sigma_g^-$ triplet ground state of the O_2 molecule.[1] Transitions between any of these three states are forbidden for the isolated molecule by selection rules for electric dipole radiation. However, perturbations caused by collisions with other molecules lead to an increase of the probability of the radiative transitions and, more importantly, open access to radiationless deactivation paths for $O_2(^1\Sigma_g^+)$ and $O_2(^1\Delta_g)$. Physical radiationless deactivation of $O_2(^1\Delta_g)$ occurs by three different mechanisms. The fastest is spin-allowed electronic energy transfer to an acceptor molecule with a triplet state of lower energy.[2] Distinctly slower is the deactivation by quenchers of low oxidation potential via a charge-transfer mechanism.[3] The slowest is spin-forbidden electronic to vibrational (e−v) energy transfer to the quenching molecule.[4−6] This ubiquitous collision-induced process drastically reduces the $O_2(^1\Delta_g)$ lifetime τ_Δ in the condensed phase and leads to an extraordinary solvent effect on τ_Δ, spanning over 5 orders of magnitude from 3.3 μs (H_2O)[7] to 0.3 s (perfluorodecaline).[8] Hurst and Schuster discovered that the rate constant k^Δ_D of collision-induced e−v deactivation of $O_2(^1\Delta_g)$ is additively composed of rate constants k^Δ_{XY} of deactivation by single terminal bonds X−Y of the quencher.[4] We found an exponential correlation of k^Δ_{XY} with the fundamental energy E_{XY} of the X−Y stretching vibration.[6] Furthermore, the importance of overtone excitations of X−Y for the overall deactivation process was documented by our comparative experiments with $^{16}O_2(^1\Delta_g)$ and $^{18}O_2(^1\Delta_g)$.[9] All these findings are comprised in a model, which calculates the probabilities of all possible coupled vibronic $O_2(^1\Delta_g, v = 0 \rightarrow {}^3\Sigma_g^-, v = m)$ and vibrational $X-Y(v' = 0 \rightarrow v' = n)$ transitions and which quantitatively reproduces the broad variation of k^Δ_{XY} values.[9]

The radiationless deactivation is by several orders of magnitude faster for $O_2(^1\Sigma_g^+)$ than for $O_2(^1\Delta_g)$, since for $O_2(^1\Sigma_g^+)$ a spin-allowed route for deactivation to $O_2(^1\Delta_g)$ exists.[10] Actually, the efficiency of $O_2(^1\Delta_g)$ formation in the quenching of $O_2(^1\Sigma_g^+)$ was found to be unity,[11,12] indicating much smaller rate constants for the direct spin-forbidden deactivation $^1\Sigma_g^+ \rightarrow {}^3\Sigma_g^-$. Most data on the quenching of $O_2(^1\Sigma_g^+)$ have been obtained in the gas phase by flow techniques.[10] The scatter of the resulting rate constants k^Σ_D determined in different laboratories approaches a variation up to a factor of 4.5, which reveals a considerable uncertainty of the gas-phase data.[13] More consistent data can be obtained in time-resolved measurements of the $^1\Sigma_g^+ \rightarrow {}^3\Sigma_g^-$ emission. Until now the only liquid-phase rate constants k^Σ_D have been reported by us.[14] These few data are mostly larger than the corresponding gas-phase rate constants, which could be a consequence of the larger normalized collision frequency of the colliding molecules in the liquid phase.

To get a broader set of data of comparable and rather low experimental uncertainty, we determined in time-resolved measurements of $O_2(^1\Sigma_g^+)$ in solution values of k^Σ_D for a larger number of quenchers. The quenchers were chosen to allow the evaluation of rate constants k^Σ_{XY} for a maximum possible number of different terminal bonds X−Y. As will be shown below, these data can in turn be used for the calculation of rate constants k^Σ_D for quenchers, which have not yet been investigated experimentally.

Experimental Details

C_2Cl_4 (99+%), $C_{10}F_{18}$ (perfluorodecaline, 95%), $C_2F_3Cl_3$ (99+%), C_6F_6 (99%), C_6H_6 (99+%), C_6H_{12} (99.5%), $CHCl_3$ (99.8%), CH_3CN (99.5%), $(CH_3)_2CO$ (99+%), CH_3OH (99.9%), CS_2 (99+%), $CDCl_3$ (99.8%), CD_2Cl_2 (99.6%), CD_3CN (99.5%), CD_3OD (99.5%), all from Aldrich, C_6D_6 (99.6%), $(CD_3)_2CO$ (99.8%), both from Deutero GmbH, $C_6F_{13}I$ (Fluka, 98+%), and CCl_4 (Janssen, 99+%) were additionally purified by column chromatography (Al_2O_3). H_2O was purified by distillation, $C_2H_4(NH_2)_2$ (ethylenediamine, Aldrich, 99+%) by crystallization. D_2O (Aldrich, 99.96%) was used as received. The singlet oxygen sensitizer phenalenone (PHE, Aldrich, 97%) was purified by column chromatography (CH_2Cl_2/silica gel).

The setup for the time-resolved measurement of the b → X phosphorescence (765 nm) and the measurement of the b → a fluorescence (1926 nm) of O_2, which both can be observed simultaneously, has been described.[12,14,15] As the excitation source we used either a short pulse (3 ns, 308 nm) excimer laser MG02 (Radiant Dyes, Wermelskirchen), a N_2-filled excimer laser (7 ns, 337 nm, EMG 101E Lambda Physik), or a dye laser FL 3002 (15 ns, 400 nm) which was pumped by an EMG 200 E excimer laser (both from Lambda Physik). As detectors served a photomultiplier R1464 (Hamamatsu) with interference filter (IF 764 nm, half-bandwidth, hbw = 19 nm)

S1089-5639(98)01170-0 CCC: $15.00
Published on Web 05/28/1998

TABLE 1: Experimental Rate Constants k^{Σ}_{D} of Deactivation of $O_2(^1\Sigma_g^+)$ by Different Quenchers Q, Experimental Uncertainty ±15%

Q	k^{Σ}_{D}/M^{-1} s^{-1}	k^{Σ}_{D}/M^{-1} s^{-1} [a]	Q	k^{Σ}_{D}/M^{-1} s^{-1}	k^{Σ}_{D}/M^{-1} s^{-1} [a]
CCl_4	7.3×10^5	6.4×10^5	H_2O	2.2×10^9	3.0×10^9
C_2Cl_4	5.5×10^5	6.4×10^5	CH_3OH	2.2×10^9	1.8×10^9
C_6F_6	9.2×10^6		$C_2H_4(NH_2)$	2.3×10^9	
$C_{10}F_{18}$	9.3×10^6	1.0×10^7	CS_2	3.2×10^6	
$C_6F_{13}I$	6.4×10^6	7.3×10^6	C_6D_6	3.2×10^8	
$C_2F_3Cl_3$	2.5×10^6	2.2×10^6	CD_2Cl_2	5.5×10^7	6.7×10^7
C_6H_6	6.6×10^8 [b]		$CDCl_3$	3.6×10^7	3.4×10^7
C_6H_{12}	1.3×10^9 [b]	1.2×10^9	CD_3CN	8.5×10^7	9.9×10^7
$CHCl_3$	6.8×10^7 [b]	1.0×10^8	$(CD_3)_2CO$	2.5×10^8	2.0×10^8
CH_3CN	3.9×10^8 [b]	3.0×10^8	D_2O	4.3×10^8	5.5×10^8
$(CH_3)_2CO$	6.0×10^8 [b]	6.1×10^8	CD_3OD	4.3×10^8	3.7×10^8

[a] From the average experimental rate constants k^{Σ}_{XY} of Table 2 recalculated values. [b] Already published data.

for time-resolved measurement of $O_2(^1\Sigma_g^+)$ and a liquid N_2-cooled InAs diode J12-D with preamplifier PA7 (EG&G Judson) equipped with IF 1940 nm, hbw = 70 nm, for intensity measurements of $O_2(^1\Sigma_g^+)$. The very fast decaying fluorescence of impurities of PHE and solvent was separated from the extremely weak but slowly decaying phosphorescence of O_2-$(^1\Sigma_g^+)$ by means of a difference technique, comparing the emissions of otherwise identical solutions of PHE with and without complete quencher of $O_2(^1\Sigma_g^+)$.[12,14] All emission experiments were averaged over 128 laser shots. Experiments were done with air-saturated solutions at room temperature, varying the laser pulse energy. Only energy-independent results are reported. The radiative deactivation of $O_2(^1\Sigma_g^+)$ by the b → a and the b → X emissions occurs in CCl_4 with rate constants $k_{b-a} = 3.4 \times 10^3$ s^{-1} and $k_{b-X} = 0.4$ s^{-1} and can thus be neglected compared with the fast radiationless deactivation.[15] Solutions were prepared and filled into sample cells in a glovebox under dry atmosphere. Values of k^{Σ}_{D} were determined for CCl_4, C_2Cl_4, and $C_2F_3Cl_3$ from the experimental $O_2(^1\Sigma_g^+)$ lifetimes τ_{Σ} in the pure solvents. For the rest of the quenchers Q the dependence of τ_{Σ} on the concentration [Q] was measured in CCl_4 solution and k^{Σ}_{D} was obtained as slope from plots of $1/\tau_{\Sigma}$ vs [Q]. For the stronger quenchers ($k^{\Sigma}_{D} > 3 \times 10^7$ M^{-1} s^{-1}) k^{Σ}_{D} was additionlly evaluated from Stern−Volmer plots of the dependence of the $O_2(^1\Sigma_g^+)$ fluorescence intensity on [Q], which was measured at 1940 nm.

Results

The lifetime of $O_2(^1\Sigma_g^+)$ reaches a maximum value of 180 ns in C_2Cl_4, exceeding the hitherto known maximum of 130 ns in CCl_4.[14,16] Table 1 lists the experimental values of k^{Σ}_{D} determined in the liquid phase. Maximum rate constants can be found for molecules containing O−H and N−H bonds, which have the highest vibrational energies. Much lower rate constants are found for perhalogenated quenchers. k^{Σ}_{D} increases in the series $CHCl_3$, CH_3CN, $(CH_3)_2CO$, C_6H_{12} proportional to the number of C−H bonds. These findings are strong evidence that these quenchers deactivate $O_2(^1\Sigma_g^+)$ by e−v energy transfer.[4,9,14,17] Thus, it is meaningful to calculate rate constants of deactivation of $O_2(^1\Sigma_g^+)$ by single terminal bonds X−Y via eq 1, where N_{XY} is the number of bonds X−Y of the quenching

$$k^{\Sigma}_{D} = \sum_{XY} N_{XY} k^{\Sigma}_{XY} \qquad (1)$$

molecule.

Rate constants $k^{\Sigma}_{CCl} = 1.8 \times 10^5$ and 1.4×10^5 M^{-1} s^{-1} are obtained from k^{Σ}_{D} of CCl_4 and C_2Cl_4, respectively. The average value $k^{\Sigma}_{CCl} = 1.6 \times 10^5$ M^{-1} s^{-1} is given in Table 2. k^{Σ}_{D} of C_6F_6 leads to the value $k^{\Sigma}_{CFar} = 1.5 \times 10^6$ M^{-1} s^{-1} for aromatically bound C−F. k^{Σ}_{D} of $C_{10}F_{18}$ yields a first value of $k^{\Sigma}_{CF} = 5.2 \times 10^5$ M^{-1} s^{-1} for aliphatically bound C−F. $k^{\Sigma}_{CF} = 4.9 \times 10^6$ M^{-1} s^{-1} is obtained from k^{Σ}_{D} of $C_6F_{13}I$, if it is considered that the deactivation by C−I cannot compete with the deactivation by C−F because of the much smaller stretching vibrational energy E_{XY} of the C−I bond. Finally, from k^{Σ}_{D} of $C_2F_3Cl_3$ we calculate $k^{\Sigma}_{CF} = (2.5 \times 10^6 - 3 \times 1.6 \times 10^5)/3 = 6.8 \times 10^5$ M^{-1} s^{-1}. The mean value $k^{\Sigma}_{CF} = 5.6 \times 10^5$ M^{-1} s^{-1} is given in Table 2. k^{Σ}_{CF} is much larger than k^{Σ}_{CCl} because of the distinctly larger energy of the stretching vibration of C−F compared with that of C−Cl, allowing a better e−v energy transfer. For the radiationless deactivation of $O_2(^1\Delta_g)$ the sequence is just opposite: $k^{\Delta}_{CCl} = 0.18$, $k^{\Delta}_{CF} = 0.049$ M^{-1} s^{-1}.[9] The reason for this deviation lies in the spin-forbiddeness of the $^1\Delta_g \rightarrow {}^3\Sigma_g^-$ deactivation, which becomes weaker in collisions with heavier atoms (Cl instead of F) and surmounts the effect of the vibrational energy dependence of the e−v deactivation of $O_2(^1\Delta_g)$.[9,18] All rate constants k^{Σ}_{XY} of Table 2 are calculated in the way described above. The inspection of the data reveals a distinct H/D isotope effect on k^{Σ}_{XY} only for O−H/O−D (factor of 6). For C−H/C−D the isotope effect is small (factor of 2 to 3). A very different behavior was found for the deactivation of $O_2(^1\Delta_g)$ where for O−H/O−D as well as for C−H/C−D the isotope effect is about a factor of 20.[9,19−22]

TABLE 2: Experimental Rate Constants k^{Σ}_{XY} of Deactivation of $O_2(^1\Sigma_g^+)$ by Terminal Bonds X−Y, Energies E_{XY} and Anharmonicty Constants x of the Highest Energy Stretching Vibration of the Deactivating Bonds X−Y, and Calculated Rate Constants $k^{\Sigma,c}_{XY}$

X−Y	k^{Σ}_{XY}/M^{-1} s^{-1} [a]	k^{Σ}_{XY}/M^{-1} s^{-1} [b]	E_{XY}	x	$k^{\Sigma,c}_{XY}$/M^{-1} s^{-1}
O−H	1.5×10^9	1.5×10^9	3755	0.024	7.7×10^8
N−H	4.7×10^8	2.8×10^8	3335	0.024	2.0×10^8
O−D	2.7×10^8	1.9×10^8	2790	0.017	1.3×10^8
C−H_{ar}	1.1×10^8	6.5×10^7	3060	0.022	8.6×10^7
C−H	1.0×10^8	3.7×10^7	2960	0.022	7.2×10^7
C−D_{ar}	5.3×10^7		2270	0.016	7.0×10^7
C−D	3.3×10^7	1.3×10^7	2250	0.017	6.5×10^7
C−S	1.6×10^6	8.5×10^5	1520	0.010	3.9×10^6
C−F_{ar}	1.5×10^6		1520	0.008	3.2×10^6
C−F_{al}	5.6×10^5	3.6×10^5	1250	0.007	1.0×10^6
C−Cl	1.6×10^5	6.8×10^4	800	0.007	2.4×10^5

[a] Liquid phase. [b] Gas phase.[13]

The average values of k^{Σ}_{XY} of Table 2 can in turn be used to recalculate the rate constant k^{Σ}_{D} of e−v deactivation of $O_2(^1\Sigma_g^+)$ by eq 1. The good agreement of the calculated values of k^{Σ}_{D} given in Table 1 with the experimental data demonstrates the accuracy of the additivity concept. Thus, eq 1 and the experimental data of k^{Σ}_{XY} can well be used to predict rate constants of e−v deactivation of $O_2(^1\Sigma_g^+)$ by quenchers, which have not yet been investigated. At this point it should be mentioned that, in contrast to $O_2(^1\Delta_g)$, deactivation of $O_2(^1\Sigma_g^+)$

seems to occur neither by chemical reactions nor by charge-transfer interactions.[23,24]

Table 2 compares the values of k^{Σ}_{XY} determined in the liquid phase with corresponding data, which have been evaluated in a previous analysis of values of k^{Σ}_{D} measured in the gas phase.[13] With exception of O−H, distinctly larger rate constants are obtained from the liquid-phase data. On average, they are larger than the gas-phase values by a factor of 2. This finding is in qualitative agreement with the results of earlier studies on the e−v deactivation of $O_2(^1\Delta_g)$ by O_2, where the rate constant in the condensed phase exceeds the gas-phase rate constant by factors of 3 (perhalogenated solvents)[8] and 1.34 (liquid O_2, 150 K),[25] respectively. The reason for this graduation is the increase of the normalized collision frequency in going from the gas to the liquid phase.[25,26] In addition, Table 2 lists the energies E_{XY} of the highest energy stretching vibration of the deactivating bonds X−Y and the corresponding anharmonicity constants x.[9]

Discussion

Model of e−v Energy Transfer. The rate constants of deactivation of $O_2(^1\Delta_g)$ by e−v energy transfer to terminal bonds X−Y could quantitatively be reproduced by us by calculating the probabilities for all possible combinations of coupled vibronic $O_2(^1\Delta_g, v = 0 \rightarrow {}^3\Sigma_g^-, v = m)$ and vibrational X−Y($v' = 0 \rightarrow v' = n$) transitions. Hereby we found already a very satisfying agreement with the experimental results, if we assume that only the highest frequency stretching vibrational mode of X−Y contributes to deactivation.[9] The reason for the validity of this very simplifying concept lies in the strong exponential increase of k^{Δ}_{XY} with the fundamental energy E_{XY} of the X−Y stretching vibration.[6] Since the liquid-phase values of k^{Σ}_{XY} also correlate roughly exponentially with E_{XY}, the same concept can be used for the quantitative interpretation of the e−v deactivation of $O_2(^1\Sigma_g^+)$, as was already shown by us in the analysis of the gas-phase rate constants k^{Σ}_{XY}.[13]

In the following discussion the model for calculation of rate constants of e−v energy transfer is briefly presented. Radiationless deactivation of $O_2(^1\Sigma_g^+)$ leads to the next lower singlet state $^1\Delta_g$.[12] We assume that deactivation proceeds only by excitation of the highest energy vibrational mode of X−Y, whereby overtone excitations of X−Y explicitly are considered. Equation 2 describes the possible coupled transitions, where m and n are the vibrational quantum numbers of O_2 and X−Y in the respective product states and E_{mn} is the corresponding off-resonance energy.

$$^1\Sigma_g^+, v = 0 + X{-}Y(v' = 0) \rightarrow {}^1\Delta_g, v = m + X{-}Y(v' = n) + E_{mn} \quad (2)$$

E_{mn} is the difference between the vibronic transition energy $E_{O2,m}$ of O_2 and the vibrational transition energy $E_{XY,n}$ of oscillator X−Y.

$$E_{mn} = E_{O2,m} - E_{XY,n} \quad (3)$$

The rate constant for the single coupled transition described by eq 2 is given by eq 4.

$$k^{mn}_{XY} = C_{\Sigma} F_m F_n' R_{mn} \quad (4)$$

Here C_{Σ} is a constant, F_m and F_n' are the Franck−Condon (FC) factors of the corresponding coupled transitions and R_{mn} is the off-resonance factor, describing the dependence of the probability of the coupled transition on E_{mn}. The off-resonance energy E_{mn} has to be accepted or provided simultaneously with the coupled transition by low-energy modes of the entire quenching molecule. Theoretical calculations for simple model systems lead to an approximately exponential relation.[27,28] Thus, we obtain for exothermic energy transfer ($E_{mn} > 0$) eq 5, where α is a measure for the ability of the quencher to accept E_{mn}. It was shown that α can be taken constant in a first approximation.[6,9] We assume that in the case of endothermic coupled transitions the effectivity of the quencher for the reverse energy flow is the same. If furthermore the availability of energy is considered by the Boltzmann factor, eq 6 results for endothermic energy transfer with gas constant R and temperature T.

$$E_{mn} > 0: \; R_{mn} = \exp(-\alpha E_{mn}) \quad (5)$$

$$E_{mn} < 0: \; R_{mn} = \exp(E_{mn}(\alpha + 1/(RT))) \quad (6)$$

Since the energy gap between the lowest excited singlet states of O_2 is small, deactivation of $O_2(^1\Sigma_g^+)$ can only lead to the vibrational levels $v = 0$, 1, 2, and 3 of the $^1\Delta_g$ state with corresponding transition energies $E_{O2,m}$ of 5239, 3755, 2297, and 865 cm^{-1}. The overall rate constant $k^{\Sigma,c}_{XY}$ is calculated by eq 7, where n_{max} is the vibrational quantum number of the highest overtone of X−Y that can be excited.

$$k^{\Sigma,c}_{XY} = \sum_{m=0}^{3} \sum_{n=1}^{n_{max}} k^{mn}_{XY} \quad (7)$$

For the calculation of $k^{\Sigma,c}_{XY}$, values of F_m, F_n' and $E_{XY,n}$ are required. The FC factors of the $^1\Delta_g$, $v = 0 \rightarrow {}^3\Sigma_g^-$, $v = m$ transitions could be calculated by an empirical relation, which was adjusted to the experimental value of F_1.[9] Unfortunately, no experimental values of FC factors of the $^1\Sigma_g^+$, $v = 0 \rightarrow {}^1\Delta_g$, $v = m$ transitions are known. However, because of the similar graduations in internuclear distance (1.23/1.22 vs 1.22/1.21), fundamental vibrational energy (1404/1484 vs 1484/1556), and anharmonicity constant (0.010/0.0085 vs 0.0085/0.0076), it can well be assumed that the values $F_0 = 1$, $F_1 = 3.0 \times 10^{-2}$, $F_2 = 4.5 \times 10^{-4}$, and $F_3 = 4.5 \times 10^{-6}$ determined for the vibronic transitions of $O_2(^1\Delta_g)$ may also be used for the vibronic transitions of $O_2(^1\Sigma_g^+)$. The derivation of eqs 8 and 9, necessary to obtain realistic overtone energies $E_{XY,n}$ and FC factors F_n' of the vibrational transitions X−Y ($v' = 0 \rightarrow v' = n$) is already described.[9]

$$E_{XY,n} = \frac{E_{XY}(n(1 - x(n+1))}{1 - 2x} \quad (8)$$

$$F_n' = \frac{E_{XY}\, n(x^{-1} - 2)\,(x^{-1} - 2n - 1)n!\,(x^{-1} - 2 - n)!}{E_{XY,n}(x^{-1} - 3)\,(x^{-1} - 2)!} \quad (9)$$

Comparison of Calculated and Experimental Results. Using the data of $E_{O2,m}$, $E_{XY,n}$, F_m, and F_n' and eqs 3−7 it is possible to calculate rate constants $k^{\Sigma,c}_{XY}$ which can be fitted to the experimental data k^{Σ}_{XY} by means of the parameters C_{Σ} (eq 4) and α (eqs 5 and 6). α is a measure of the ability of the entire quenching molecule to accept or to supply the off-resonance energy simultaneously with the coupled transition via low-energy vibrational and rotational modes. In the previous quantitative analysis of the liquid-phase rate constants k^{Δ}_{XY} of e−v deactivation of $O_2(^1\Delta_g)$ by X−Y it was found that the constant $\alpha = 0.0032\ (cm^{-1})^{-1}$ can be taken as a general value for polyatomic quenchers. Since the quencher's ability to accept or to supply the off-resonance energy will certainly not depend

on the excited state of O_2, the same value of $\alpha = 0.0032$ $(cm^{-1})^{-1}$ should be a general parameter in the e−v deactivation of $O_2(^1\Sigma_g^+)$ too. Thus, already a *one-parameter fit* should be sufficient to describe the experimental results for $O_2(^1\Sigma_g^+)$.

The fit parameter C_Σ can be interpreted as the product of the normalized collision frequency of the colliding pair in the liquid-phase Z_l with the electronic factor f_Σ of the $^1\Sigma_g^+ \rightarrow {}^1\Delta_g$ transition of O_2, and with a steric factor s: $C_\Sigma = Z_l f_\Sigma s$. Only f_Σ is independent of the molecular properties of the quencher. Z_l is assumed to be larger than the normalized collision frequency Z_g in the gas phase by the value of the pair distribution function $g(\sigma)$ at contact distance σ.[25,26] If the model of hard spheres is applied to the liquid phase, then the value of $g(\sigma)$ depends on the packing fraction of the solvent but also on the diameters of the spherically assumed O_2, solvent, and quencher molecules.[29,30] Z_g depends via the collision distance and the reduced mass of the colliding pair on the size and mass of the quencher, and s, which describes the accessibility of O_2 to the deactivating bond in collinear collisions, depends on the molecular structure of quencher. The fact that we use one general value of C_Σ for the calculation of $k^{\Sigma,c}_{XY}$ represents therefore a strong simplification. Since variations in Z_l and s will only fortuitously compensate each other, a scatter of k^{Σ}_{XY} around the calculated data $k^{\Sigma,c}_{XY}$ has to be expected as was already found in the treatment of the k^{Δ}_{XY} data.

The last column of Table 2 collects the values of $k^{\Sigma,c}_{XY}$ calculated with the above-described model and with $C_\Sigma = 2.0 \times 10^{10}$ M^{-1} s^{-1}. The comparison with the experimental rate constants demonstrates that the large variation of k^{Σ}_{XY} over 4 orders of magnitude is in principle reproduced. Calculated and experimental rate constants differ at maximum by a factor of 2.4. A similarly large maximum deviation has already been stated in the analysis of the e−v deactivation of $O_2(^1\Delta_g)$ which requires the fit parameter $C_\Delta = Z_l f_\Delta s = 5.5 \times 10^5$ M^{-1} s^{-1}.[9]

To improve the agreement between the experimental data and the calculation for the deactivation of $O_2(^1\Sigma_g^+)$, we tried to consider the quencher-dependent variation of the collision frequency. We first normalized the experimental data to a common collision frequency by calculating k^{Σ}_D/Z_l before we calculated incremental rate constants of deactivation by X−Y. However, the agreement between these normalized incremental rate constants and the rate constants obtained from the e−v energy transfer model with a common value of C_Σ was not better. Possibly, the failure of improvement was caused by the neglect of variation of the steric factor s. Most probably, however, a further improvement was prohibited by the rather crude approximative equations for the value $g(\sigma)$ of the pair distribution function at contact distance.[25,26,29]

Figure 1 demonstrates the quality of the model for the e−v deactivation of both $O_2(^1\Delta_g)$ and $O_2(^1\Sigma_g^+)$ by means of the comparison of experimental and calculated rate constants in a double logarithmic plot. The data of k^{Δ}_{XY} and $k^{\Delta,c}_{XY}$ have been taken from our earlier work.[9,31]

The straight line represents identity of experimental and calculated rate constants. Actually, the linear least-squares fit to all liquid-phase data yields the slope 1.00 ± 0.02 and the intercept 0.00 ± 0.30. The reproduction of the experimental data by the model is impressive, if one considers the broad variation of rate constants spanning over more than 10 orders of magnitude. The gas-phase data k^{Σ}_{XY} show a slightly stronger deviation from the fit, which could be caused by a larger experimental uncertainty.

Figure 2 shows the correlations of $\log(k^{\Sigma}_{XY})$ and $\log(k^{\Delta}_{XY})$ with E_{XY}. $\log(k^{\Delta}_{XY})$ increases much stronger with E_{XY} than

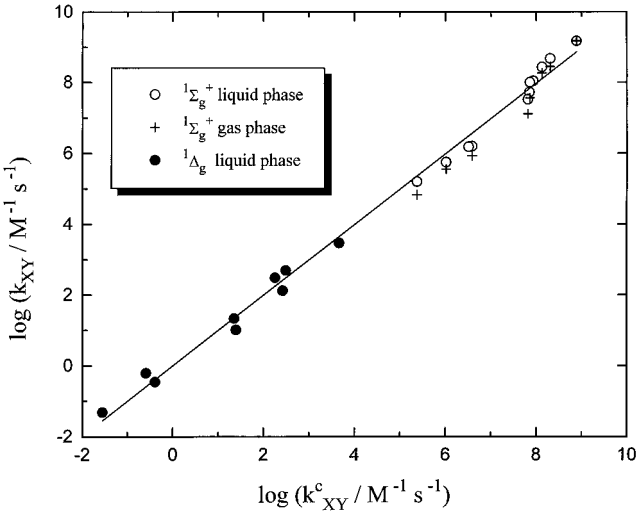

Figure 1. Correlation of experimental and calculated rate constants of e−v deactivation of $O_2(^1\Sigma_g^+)$ and $O_2(^1\Delta_g)$ by terminal bonds X−Y. Straight line represents linear fit and identity.

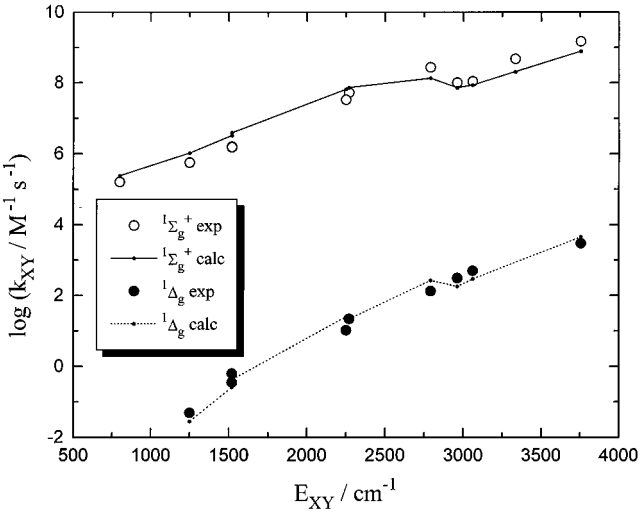

Figure 2. Logarithmic plot of experimental and calculated rate constants of e−v deactivation of $O_2(^1\Sigma_g^+)$ and $O_2(^1\Delta_g)$ by terminal bonds X−Y versus the corresponding energy E_{XY}.

$\log(k^{\Sigma}_{XY})$ as a consequence of the larger energy gap for the corresponding deactivation process (7882 vs 5239 cm^{-1}).

Furthermore, Figure 2 reveals that the values of $\log(k^{\Sigma,c}_{XY})$ increase more slowly with E_{XY} than the experimental data: they are systematically larger than $\log(k^{\Sigma}_{XY})$ for small energies E_{XY}, but smaller for large energies E_{XY}; see also Table 2. For $O_2(^1\Delta_g)$, however, no systematic deviation of $\log(k^{\Delta,c}_{XY})$ from $\log(k^{\Delta}_{XY})$ is observed. This different behavior points to the limitations of the model due to the simplifying assumption that only excitation of the stretching vibration of the bond X−Y contributes to e−v deactivation. Bending vibrations of X−Y and perhaps combinational modes of the entire quenching molecule could of course also couple to vibronic transitions of O_2 and thus induce deactivation of singlet oxygen. However, since for O−H, N−H, C−H, and O−D the energy of the bending mode is only about half of E_{XY}, the probability of deactivation by excitation of bending vibrations is expected to be much lower than that by stretching vibrations. This obviously holds true for $O_2(^1\Delta_g)$, for which $\log(k^{\Delta}_{XY})$ increases strongly with E_{XY} because of the large energy gap of 7882 cm^{-1}. For $O_2(^1\Sigma_g^+)$, however, the increase of $\log(k^{\Sigma}_{XY})$ with E_{XY} is much weaker due to the smaller energy gap of 5239 cm^{-1}. Therefore,

the rate constant of $O_2(^1\Sigma_g^+)$ deactivation by coupling to a bending mode of X−Y can no more be expected to be negligible compared with the rate constant of deactivation by coupling to the stretching mode of the same bond. However, since they are not considered in the calculation, deviations of $k^{\Sigma,c}_{XY}$ to smaller values result for bonds X−Y with high energies E_{XY}.

The neglect of deactivation by excitation of bending modes of bonds X−Y is certainly also one reason for the less satisfying agreement of calculated and experimental rate constants found in the analysis of the deactivation of the isoelectronic $^1\Sigma^+$ excited molecules NF, PF, NCl, and PCl with the present model for e−v energy transfer, since in these cases the $^1\Sigma^+ - ^1\Delta$ energy gap is likewise rather small.[32−35]

Most of the rate constants k^{Σ}_{XY} and k^{Δ}_{XY} have been evaluated from similar sets of liquid-phase data k^{Σ}_{D} and k^{Δ}_{D}. Therefore, the average values of products Z_ls contained in the fit parameters C_Σ and C_Δ can be assumed to be approximately the same, and the ratio $C_\Sigma/C_\Delta = 3.7 \times 10^4$ can be identified as the ratio f_Σ/f_Δ of the electronic factors of spin-allowed and spin-forbidden e−v deactivation of singlet oxygen. Thus, the relative forbiddeness of the collision-induced intersystem crossing is much weaker for O_2 than for aromatic hydrocarbons, for which the ratio of electronic factors of intersystem crossing and internal conversion is about $f_{TS}/f_{SS} = 10^{-8}$.[36]

The ratio f_Σ/f_Δ is smaller than the ratio $k^{\Sigma}_{XY}/k^{\Delta}_{XY}$, which increases from about 5×10^5 (O−H) to 1×10^7 (C−F), indicating that the smaller rate constants of e−v deactivation of $O_2(^1\Delta_g)$ are to some degree also the consequence of the larger corresponding energy gap. The rate constants of e−v energy transfer decrease strongly with further increasing energy gap. The excitation energy of $O_2(^1\Sigma_g^+)$ amounts to 13 121 cm^{-1}. Even if we assume the same favorable electronic factor as for the $^1\Sigma_g^+ \rightarrow {}^1\Delta_g$ deactivation, the model calculates for the $^1\Sigma_g^+ \rightarrow {}^3\Sigma_g^-$ e−v deactivation of $O_2(^1\Sigma_g^+)$ only very small rate constants ranging from 2×10^2 (O−H) to 7×10^{-5} (C−F) $M^{-1}\ s^{-1}$, which are by several orders of magnitude smaller than the corresponding data for k^{Σ}_{XY}; see Table 2. Of course, even smaller rate constants result with a smaller corresponding electronic factor. Thus, the effect of the energy gap on the magnitude of the rate constants is already large enough to explain, without referring to spin-forbiddenness, why $O_2(^1\Delta_g)$ is the only product of the e−v deactivation of $O_2(^1\Sigma_g^+)$.[12]

Comparison of Collision-Induced Radiationless and Radiative Deactivation. Parallel to the above-discussed radiationless deactivation processes of singlet oxygen the radiative transitions a → X and b → a occur, which are also strongly increased by perturbations caused in collisions. Whereas for the isolated O_2 molecule $k_{a-X} = 2.6 \times 10^{-4}\ s^{-1}$ and $k_{b-a} = 2.5 \times 10^{-3}\ s^{-1}$ have been determined,[37,38] much larger rate constants of $k_{a-X} = 1.27 \times 10^{-2}\ s^{-1}$ and $k_{b-a} = 41\ s^{-1}$ have been found in a solid Ar matrix.[39] The rate constants are even larger in liquid CCl_4 at room temperature, where we measured $k_{a-X} = 1.1\ s^{-1}$ and $k_{b-a} = 3.4 \times 10^3\ s^{-1}$.[15] Equation 10 allows the

$$\frac{k_{b-a}}{k_{a-X}} = \frac{(f_{b-a}/f_{a-X})(E_\Sigma - E_\Delta)^3}{E_\Delta{}^3} \qquad (10)$$

calculation of the ratio of the electronic factors f_{b-a}/f_{a-X} of spin-allowed and spin-forbidden collision-induced radiative deactivation of singlet oxygen.

From both the Ar matrix and the liquid CCl_4 data we obtain as ratio of the electronic factors of the collision-induced radiative transitions $f_{b-a}/f_{a-X} = 1.1 \times 10^4$. According to a theory developed by Minaev the b → a radiative transition gains intensity in collisions due to an asymmetric charge transfer from the colliding molecule to the molecular orbitals of O_2, which induces electric dipole character into the transition. Because of the rather large spin−orbit coupling between the $b^1\Sigma_g^+$ and $X^3\Sigma_g^-$ states the a → X transition profits from the increase of k_{b-a}. Thus, the value of f_{b-a}/f_{a-X} is already determined by the value of the spin−orbit coupling constant of the oxygen atom.[40] Actually, the theory of Minaev was quantitatively proved by us.[15] The ratio $f_{b-a}/f_{a-X} = 1.1 \times 10^4$ is not very different from the ratio $f_\Sigma/f_\Delta = 3.7 \times 10^4$ of the electronic factors of the collision-induced radiationless transitions. This result indicates that spin−orbit coupling plays also an important role in the relation between spin-forbidden and spin-allowed e−v deactivation of $O_2(^1\Delta_g)$ and $O_2(^1\Sigma_g^+)$.

Conclusions

Rate constants k^{Σ}_{D} have been determined for 22 different quenchers. As we have shown it is possible to calculate, from the set of experimental k^{Σ}_{XY} data, values of k^{Σ}_{D} for quenchers, which have not yet been investigated. Liquid-phase rate constants k^{Σ}_{D} are by a factor of ≈2 larger than the corresponding gas-phase rate constants. The difference can qualitatively be explained with the larger collision frequency in the liquid phase.

The radiationless deactivation of $O_2(^1\Sigma_g^+)$ proceeds via e−v energy transfer to a single terminal bond X−Y of the quenching molecule. The same kind of energy transfer operates in the ubiquitous collisional deactivation of $O_2(^1\Delta_g)$. The huge variation of the corresponding rate constants over more than 10 orders of magnitude is impressively well reproduced by the e−v transfer model of coupled vibronic and vibrational transitions of O_2 and X−Y, although only the excitation of the stretching mode of X−Y is considered. If only the data of $O_2(^1\Sigma_g^+)$ are analyzed, limititations due to this simplification become obvious. A better quantitative reproduction of rate constants would probably result from the additional inclusion of the excitation of bending modes of X−Y into the e−v deactivation model. However, the necessary general data about vibrational energies, anharmonicity constants, and FC factors of bending vibrations are missing. On the basis of the present model of e−v energy transfer, we have demonstrated that the large difference in energy gaps of 13 121 cm^{-1} vs 5239 cm^{-1} is the main reason for the ineffectiveness of the $^1\Sigma_g^+ \rightarrow {}^3\Sigma_g^-$ e−v deactivation compared with the $^1\Sigma_g^+ \rightarrow {}^1\Delta_g$ e−v deactivation of $O_2(^1\Sigma_g^+)$.

The ratio $f_\Sigma/f_\Delta = 3.7 \times 10^4$ of the electronic factors of the e−v deactivation processes $^1\Sigma_g^+ \rightarrow {}^1\Delta_g$ and $^1\Delta_g \rightarrow {}^3\Sigma_g^-$ was found to be very similar to the ratio f_{b-a}/f_{a-X} of the corresponding collision-induced radiative transitions. This result indicates that spin−orbit coupling plays also an important role in the relation between spin-forbidden and spin-allowed e−v deactivation of $O_2(^1\Delta_g)$ and $O_2(^1\Sigma_g^+)$.

Acknowledgment. Financial support by the Deutsche Forschungsgemeinschaft and the Fonds der Chemischen Industrie is gratefully acknowledged.

References and Notes

(1) Herzberg, G. *Spectra of Diatomic Molecules*; Van Nostrand Reinhold: New York, 1950. We will use for the $b^1\Sigma_g^+$, $a^1\Delta_g$ and $X^3\Sigma_g^-$ states of O_2 the abbreviations $^1\Sigma_g^+$, $^1\Delta_g$, and $^3\Sigma_g^-$ in the discussion of radiationless transitions and b, a, and X in the discussion of radiative transitions.

(2) Wilkinson, F.; Ho, W.-T. *Spectrosc. Lett.* **1978**, *11*, 455.

(3) Young, R. H.; Martin, R. L.; Feriozi, D.; Brewer, D.; Kayser, R. *Photochem. Photobiol.* **1973**, *17*, 233.

(4) Hurst, J. R.; Schuster, G. B. *J. Am. Chem. Soc.* **1983**, *105*, 5756.

(5) Rodgers, M. A. J. *J. Am. Chem. Soc.* **1983**, *105*, 6201.
(6) Schmidt, R.; Brauer, H.-D. *J. Am. Chem. Soc.* **1987**, *109*, 6976.
(7) Egorov, S. Y.; Kamalov, V. F.; Koroteev, N. I.; Krasnovskii, A. A.; Toleutaev, B. N.; Zinukov, S. V. *Chem. Phys. Lett.* **1989**, *163*, 421. Using an improved setup, we were able to confirm their result $\tau_\Delta = 3.3\ \mu$s in H_2O.
(8) Afshari, E.; Schmidt, R. *Chem. Phys. Lett.* **1991**, *184*, 128.
(9) Schmidt, R.; Afshari. E. *Ber. Bunsen-Ges. Phys. Chem.* **1992**, *96*, 788.
(10) Wayne, R. P. *Singlet O_2;* Frimer, A. A., Ed.; CRC Press: Boca Raton, FL, 1985; Vol. 1, p 81.
(11) Wildt, J.; Bednarek, G.; Fink, E. H.; Wayne, R. P. *Chem. Phys.* **1988**, *122*, 1842.
(12) Schmidt, R.; Bodesheim, M. *Chem. Phys. Lett.* **1993**, *213*, 111.
(13) Schmidt, R. *Ber. Bunsen-Ges. Phys. Chem.* **1992**, *96*, 794.
(14) Schmidt, R.; Bodesheim, M. *J. Phys. Chem.* **1994**, *98*, 2874.
(15) Schmidt, R.; Bodesheim, M. *J. Phys. Chem.* **1995**, *99*, 15919.
(16) Chou, P.-T.; Wei, G.-T.; Lin, C.-H.; Wei, C.-Y.; Chang, C.-H. *J. Am. Chem. Soc.* **1996**, *118*, 3031.
(17) Wang, B.; Ogilby, P. R. *J. Phys. Chem.* **1993**, *97*, 193.
(18) Schmidt, R. *J. Am. Chem. Soc.* **1989**, *111*, 6983.
(19) Egorov, S. Y.; Krasnovsky, A. A. *Biofizika* **1983**, *28*, 497.
(20) Hurst, J. R.; McDonald, J. D.; Schuster, G. B. *J. Am. Chem. Soc.* **1982**, *104*, 2065.
(21) Ogilby, P. R.; Foote, C. S. *J. Am. Chem. Soc.* **1982**, *104*, 2069.
(22) Gorman, A. A.; Hamblett, I.; Lambert, C.; Prescott, A. L.; Rodgers, M. A. J.; Spence, H. M. *J. Am. Chem. Soc.* **1987**, *109*, 3091.
(23) Scurlock, R. D.; Wang, B.; Ogilby, P. R. *J. Am. Chem. Soc.* **1996**, *118*, 388.
(24) Bodesheim, M.; Schmidt, R. *J. Phys. Chem. A* **1997**, *101*, 5672.
(25) Chatelet, M.; Tardieu, A.; Spreitzer, W.; Maier, M. *Chem. Phys.* **1986**, *102*, 387.
(26) Einwohner, T.; Alder, B. *J. Chem Phys.* **1968**, *49*, 1548.
(27) Dickens, P. G.; Linett, J. W.; Sovers, O. *Discuss. Faraday Soc.* **1962**, *33*, 52.
(28) Hippler, H.; Schranz, H. W.; Troe, J. *J. Phys. Chem.* **1986**, *90*, 6158.
(29) Yoshimura, Y.; Nakahara, M. *J. Chem. Phys.* **1984**, *81*, 4080.
(30) Schmidt, R.; Seikel, K.; Brauer, H.-D. *J. Phys. Chem.* **1989**, *93*, 4507.
(31) For H_2O $\tau_\Delta = 3.3\ \mu$s is the correct lifetime instead of $\tau_\Delta = 4.2\ \mu$s used earlier by us. The inclusion of this value in the data basis yields $k^\Delta_{OH} = 2730$ instead of the earlier value of 2150 $M^{-1}\ s^{-1}$, which leads to an only very slight shift of the corresponding data point on the log scale of Figure 1.
(32) Schmidt, R. *J. Phys. Chem.* **1993**, *97*, 3658.
(33) Zhao, Y.; Setser, D. W. *J. Phys. Chem.* **1994**, *98*, 9723.
(34) Zhao, Y.; Setser, D. W. *J. Chem. Soc., Faraday. Trans.* **1995**, *98*, 2979.
(35) Liu, C.; Zou, S.; Guo, J.; Gu, Y.; Cao, D.; Chu, Y.; Setser, D. W. *J. Phys. Chem. A.* **1997**, *101*, 7345.
(36) Birks, J. B. *Photophysics of Aromatic Molecules*; Wiley-Interscience: New York, 1970, p 142.
(37) Badger, R. M.; Wright, A. C.; Whitlock, R. F. *J. Chem. Phys.* **1965**, *43*, 4345.
(38) Noxon, J. F. *Can. J. Phys.* **1961**, *39*, 1110.
(39) Becker, A. C.; Schurath, U.; Dubost, H.; Galaup, J. P. *Chem. Phys.* **1988**, *125*, 321.
(40) Minaev, B. F.; Lunell, S.; Kobzev, G. I. *J. Mol. Struct. (THEOCHEM)* **1993**, *284*, 1.